



Sharif University of Technology

Scientia Iranica

Transactions A: Civil Engineering

www.sciencedirect.com



Analytical approach for predicting full torsional behavior of reinforced concrete beams strengthened with FRP materials

A.R. Zojaji, M.Z. Kabir*

Department of Civil and Environmental Engineering, Amirkabir University of Technology, Tehran, P.O. Box 15875-4413, Iran

Received 2 March 2011; revised 4 October 2011; accepted 21 November 2011

KEYWORDS

Analytical model;
Torque;
Torsion;
Reinforced concrete;
FRP;
Strengthening;
Softened membrane model
for torsion.

Abstract A new computational procedure is developed to predict the full torsional response of reinforced concrete beams strengthened with Fiber Reinforced Plastics (FRPs), based on the Softened Membrane Model for Torsion (SMMT). For validating the proposed analytical model, torque-twist curves obtained from current theoretical approaches are compared with experimental ones for both solid and hollow rectangular sections. The good agreement results of this comparison show that the proposed analytical model is reliable for predicting the torsional behavior of FRP-strengthened reinforced concrete beams before and after cracking. By means of the developed approach, the power of the SMMT method, in extending to FRP-strengthened reinforced concrete beams, is demonstrated in this paper. Moreover, the contribution of FRP fabrics to the torsional response, as an external bonded reinforcement, is studied in various practical strengthening configurations. Therefore, the efficiency of each configuration is illustrated as well.

© 2012 Sharif University of Technology. Production and hosting by Elsevier B.V.

Open access under [CC BY-NC-ND license](#).

1. Introduction

Reinforced concrete members in a structure may be subjected to loads with magnitudes higher than those considered as design loads. Axial forces, shear forces, bending moments, torsion, or a combination of these effects, are considered to design a safe structural member. For most design situations, bending moments and shear forces are considered as primary effects, whereas torsion is regarded as secondary [1]. For this reason, the torsional behavior of reinforced concrete beams is not studied as much in depth as their behavior under bending and shear stresses [1]. Torsion becomes a primary effect, however, for situations such as spandrel or curved beams [2].

The torsional strengthening of RC beams has been conducted by some techniques, such as steel plate jacketing, increasing

cross sections, and adding extra steel bars. The advantages of Fiber-Reinforced-Polymers (FRPs), such as their relatively high strength to weight ratio, high resistance in corrosive regions, and their easy-to-apply character, caused engineering interest in extending the application of this material for strengthening demands [3]. While the literature on torsional strengthening is quite limited, initiated just in 2001, the flexural and shear strengthening of RC beams with FRP materials has been studied since the early 1990s [3]. Since then, flexural and shear capacity has only been included in design guides and recommendations (FIB [4], JSCE [5], ACI [6] and CSA [7]). In the case of torsional strengthening with FRP materials, only FIB proposed design equations based on shear strengthening models have been proposed [3].

Previous research on the torsional behavior of FRP-strengthened reinforced concrete beams encompassed experimental, analytical and numerical investigations. Experimental investigations on the torsional behavior of concrete beams with and without stirrups, including rectangular and T-shaped sections strengthened using FRP sheets and strips as external transverse reinforcement, have been conducted by Chaliotis [8]. An analytical model based on the softened truss model in conjunction with the smeared crack theory was then proposed by Chaliotis [3] to obtain the entire behavior of RC beams strengthened by FRP under torsion. The Chaliotis analytical model is comprised of two distinctive steps to obtain the torsional behavior of strengthened beams in pre and post cracking stages. Ghobarah et al. [2] conducted experimental tests on

* Corresponding author.

E-mail address: mzkabir@aut.ac.ir (M.Z. Kabir).



FRP-strengthened reinforced concrete beams subjected to torsion and a small value of flexure, to study the effect of various strengthening configurations with carbon and glass FRP sheets and strips. To validate their experimental tests with an analytical approach, Deifalla and Ghobarah [9] utilized the compression field theory and established a series of equations for computing the contribution of FRP sheets to the torsional resistance of beam. Ameli et al. [10] presented the results of experiments together with a numerical study on reinforced concrete beams under pure torsion that were strengthened with FRP sheets in a variety of configurations. Ameli and Ronagh [11] introduced an analytical method for evaluating the ultimate torque of FRP-strengthened reinforced concrete beams based on the compression field theory. Their computational procedure only capable of predicting the torsional strength of strengthened beams and, consequently, an entire response is not obtained. Solid and box-section reinforced concrete beams with externally-bonded CFRP strips were studied through experimental and numerical work that was carried out by Hii and Al-Mahaidi [12]. Panchacharam and Belarbi [13] studied the behavior and performance of reinforced concrete members strengthened with GFRP sheets with a variety of fiber orientation, the number of beam faces strengthened, the number of FRP plies, and the wrapping configuration during experimental tests.

According to experimental tests, strengthening with continuous FRP sheets provides more efficient confinement than that of the strip, due to less crack openings [2,8,10,13]. U-jacketing configuration was experimentally investigated in [8,10,13]. Since shear flow stresses take a circular shape during torsional load, torsion would not be well resisted in the case of U-jacketing strengthening. As expected, the torsional capacity of U-wrap strengthened beams increases less compared to full-wrap strengthened beams [8,10,13]. An experimental study on the effect of fiber orientation revealed that FRP sheets with fibers oriented parallel to the longitudinal axis of the beam would not contribute to the post-cracking stiffness of the beam [13].

The aim of this paper is to present an analytical model to obtain the full torsional behavior of reinforced concrete beams strengthened by FRP based on the Softened Membrane Model for Torsion (SMMT); a new model which has been recently proposed by Jeng and Hsu [14]. In fact, the contribution of this paper is an attempt to extend and modify the SMMT algorithm for the case of FRP strengthened beams. As yet, analytical models which have extended for FRP-strengthened RC beams are Compression Field Theory, Modified Compression Field Theory, and Softened Truss Model. Among these models, SMMT can predict the entire torque-twist curve by considering tension stress in equilibrium equations. Thanks to the proposed analytical approach, it is possible to predict the entire torsional behavior (pre-cracking and post-cracking stages) of FRP strengthened reinforced concrete beams.

The validation of SMMT for 81 experimental tests on reinforced concrete beams with steel bars and stirrups in [14] shows the high acceptable results. In the present study, this methodology is extended and properly modified in order to include the influence of FRP materials on torsional behavior as external reinforcement.

To obtain a reliable validation of the proposed model, reported experimental data available from the literature were considered collectively in an attempt to check the accuracy of the proposed method, based on test results of a range of parametric studies. Extensive comparisons between analytical

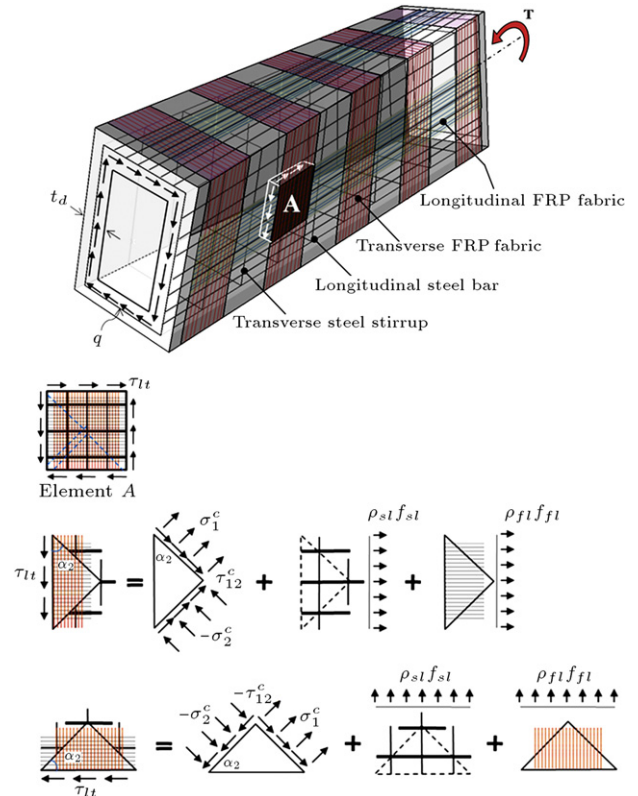


Figure 1: Torsional deformation of a FRP strengthened RC beam and in-plane stresses of an element taken from shear flow zone.

and measured data, which also include full torsional curves of reinforced concrete beams strengthened with carbon or glass FRP materials (continuous sheets and strips) in various retrofitting configurations, are also presented and discussed herein.

2. Analytical model

After concrete beams crack, torsion is then resisted by a truss action of compressive stresses in diagonal concrete struts, and tensile stresses in longitudinal bars, transverse stirrups, and FRP external reinforcement. For calculating the post-cracking torsional behavior of reinforced concrete beams strengthened by FRP, the well-known softened membrane model for torsion, which was first developed by Jeng and Hsu [14] and which is an extension of the latest shear model (SMM), is adopted and modified to include the FRP strengthening effect. In this approach, equilibrium and compatibility equations are solved in conjunction with the constitutive laws of an element taken from a member subjected to pure torsion, as shown in Figure 1. To implement the influence of the epoxy-bonded FRP materials as the external strengthening tools in the SMMT method, terms of FRP stresses are added to the equilibrium equations in longitudinal and transverse directions. Moreover, the confinement of concrete, in the case of FRP wrapping through the beam section, is considered in constitutive laws of compressive concrete. A trial-and-error algorithm was developed, based on that proposed by Jeng and Hsu [14], to calculate each point of the torque-twist curve.

2.1. Equilibrium equations

Generally, applying pure torsion on a rectangular section produces uniform shear stresses ($\tau_t = q/t_d$) on a certain

thickness of the section, called the effective shear flow zone (t_d). A reinforced concrete rectangular beam strengthened with FRP and subjected to pure torsion, T , is shown in Figure 1, which is an extension of that proposed by Jeng [15]. Considering the rectangular finite element of a FRP strengthened reinforced concrete beam from the shear flow zone (element A in Figure 1), the state of in-plane stress can be represented by Mohr's circle by defining the l - t coordinate as the direction of longitudinal and transverse steel bars, and the 2 - 1 coordinate as the direction of principal applied stresses. In this paper, the effect of FRP forces is included in equilibrium equations by considering FRP sheets as additional external reinforcements. So, in-plane equilibrium equations for the element, A, taken from a FRP strengthened RC beam, can be represented as follows:

$$\sigma_l = \sigma_2^c \cos^2 \alpha_2 + \sigma_1^c \sin^2 \alpha_2 + 2\tau_{21}^c \sin^2 \alpha_2 \cos^2 \alpha_2 + \rho_{sl} f_{sl} + \rho_{fl} f_{fl}, \quad (1a)$$

$$\sigma_t = \sigma_2^c \sin^2 \alpha_2 + \sigma_1^c \cos^2 \alpha_2 - 2\tau_{21}^c \sin^2 \alpha_2 \cos^2 \alpha_2 + \rho_{st} f_{st} + \rho_{ft} f_{ft}, \quad (1b)$$

$$\tau_{lt} = (-\sigma_2^c + \sigma_1^c) \sin \alpha_2 \cos \alpha_2 + \tau_{21}^c (\cos \alpha_2 - \sin \alpha_2), \quad (1c)$$

where, σ_l and σ_t are applied normal stresses in the longitudinal and transverse directions of the RC element, respectively, σ_1^c and σ_2^c are average normal stresses of concrete in the 1 and 2 -directions, respectively, τ_{lt} is the applied shear stress in the l - t coordinate of the steel bars, τ_{21}^c is the smeared (average) shear stress of concrete in the 2 - 1 coordinate, α_2 is the angle of applied principal compressive stress (2 -axis), with respect to the l -axis, ρ_{sl} and ρ_{st} are longitudinal and transverse steel ratios, respectively, and ρ_{fl} and ρ_{ft} are longitudinal and transverse steel ratios, respectively. Since, normal stresses in an element taken from a member under pure torsion are zero, according to the mechanics of materials, the infinitesimal element, shown in Figure 1, is in a pure shear stress state ($\sigma_l = \sigma_t = 0$), and $\alpha_2 = 45^\circ$.

The reinforced ratios used in Eq. (1) are calculated by the following expressions:

$$\rho_{sl} = \frac{A_{sl}}{p_0 t_d}, \quad (2)$$

$$\rho_{st} = \frac{A_{st} p_{st}}{p_0 t_d s}, \quad (3)$$

$$\rho_{fl} = \frac{A_{fl}}{p_0 t_d}, \quad (4)$$

$$\rho_{ft} = \frac{A_{ft} p_{ft}}{p_0 t_d s_f}, \quad (5)$$

where p_0 is the perimeter of the centerline of the shear flow ($p_0 = p_c - 4t_d$), A_{sl} is the total area of steel longitudinal bars, A_{st} is the area of the steel stirrup, p_{st} is the perimeter of the area enclosed by the stirrup, s is the spacing of the stirrups, A_{fl} and A_{ft} are the FRP areas in longitudinal and transverse directions, respectively, and p_{ft} is the perimeter of the strengthened beam cross-section by FRP in a transverse direction. Adopting Bredt's equation for an equivalent thin walled cross section, the torsional moment, T , is calculated from Eq. (6):

$$T = 2 A_0 q = 2 A_0 t_d \tau_{lt}, \quad (6)$$

where T is torsional moment, and A_0 is the area enclosed by the centerline of the shear flow ($A_0 = A_c - 0.5 p_c t_d + t_d^2$).

2.2. Compatibility equations

The in-plane compatibility of the shear element, A, of Figure 1 should satisfy the three following equations:

$$\varepsilon_l = \varepsilon_2 \cos^2 \alpha_2 + \varepsilon_1 \sin^2 \alpha_2 + \gamma_{21} \sin \alpha_2 \cos \alpha_2, \quad (7a)$$

$$\varepsilon_t = \varepsilon_2 \sin^2 \alpha_2 + \varepsilon_1 \cos^2 \alpha_2 - \gamma_{21} \sin \alpha_2 \cos \alpha_2, \quad (7b)$$

$$\frac{\gamma_{lt}}{2} = (-\varepsilon_2 + \varepsilon_1) \sin \alpha_2 \cos \alpha_2 + \frac{\gamma_{21}}{2} (\cos \alpha_2 - \sin \alpha_2), \quad (7c)$$

where ε_l and ε_t are average biaxial strains of steel bars and stirrups in the longitudinal and transverse directions, respectively, γ_{lt} is the average shear strain in the l - t coordinate of the steel bars, ε_1 and ε_2 are average biaxial strains in the 1 -direction and the 2 -direction, respectively, and γ_{21} is the average shear strain in the 2 - 1 coordinate.

Since, constitutive laws of materials are calculated from uniaxial strains, it is necessary to determine uniaxial strains with respect to biaxial ones. Hsu and Zhu [16] gave the relationships between biaxial and uniaxial strains in the following algebraic forms:

$$\bar{\varepsilon}_1 = \frac{1}{1 - \nu_{12}\nu_{21}} \varepsilon_1 + \frac{\nu_{12}}{1 - \nu_{12}\nu_{21}} \varepsilon_2, \quad (8a)$$

$$\bar{\varepsilon}_2 = \frac{\nu_{12}}{1 - \nu_{12}\nu_{21}} \varepsilon_1 + \frac{1}{1 - \nu_{12}\nu_{21}} \varepsilon_2, \quad (8b)$$

$$\bar{\gamma}_{21} = \gamma_{21}. \quad (8c)$$

ν_{12} and ν_{21} are Hsu/Zhu ratios, which are defined as [16]:

$$\nu_{12} = 0.2 + 850 \varepsilon_{sf} \quad \varepsilon_{sf} \leq \varepsilon_y, \quad (9)$$

$$\nu_{12} = 1.9 \quad \varepsilon_{sf} > \varepsilon_y,$$

$$\nu_{21} = 0, \quad (10)$$

where ε_{sf} is the average strain of the steel bars that yield first, ε_y is the yield strain of steel bars.

The average uniaxial strains in the l -direction ($\bar{\varepsilon}_l$) and the t -direction ($\bar{\varepsilon}_t$) of the steel bars are calculated by a procedure similar to Eq. (7), if uniaxial strains are replaced by biaxial ones.

Two other compatibility equations relate the angle of twist per unit length and bending curvature of the concrete to shear distortion in the wall, as follows [14]:

$$\varphi = \frac{p_0}{2A_0} \gamma_{lt}, \quad (11)$$

$$\psi = \varphi \sin 2\alpha_2 = \frac{p_0}{2A_0} \gamma_{lt} \sin 2\alpha_2. \quad (12)$$

Since the strain distribution is assumed to be linear, thickness, t_d , is calculated as [14]:

$$t_d = \frac{\bar{\varepsilon}_{2s}}{\psi}, \quad (13)$$

where:

$$\bar{\varepsilon}_{2s} = 2\bar{\varepsilon}_2.$$

Substituting ψ from the first part of Eq. (12) and the equations for computing p_0 and A_0 results in calculating t_d by the following expression [14]:

$$t_d = \frac{1}{2H + 8} \left[p_c \left(1 + \frac{H}{2} \right) - \sqrt{\left(1 + \frac{H}{2} \right)^2 p_c^2 - 4H(H + 4)A_c} \right], \quad (14)$$

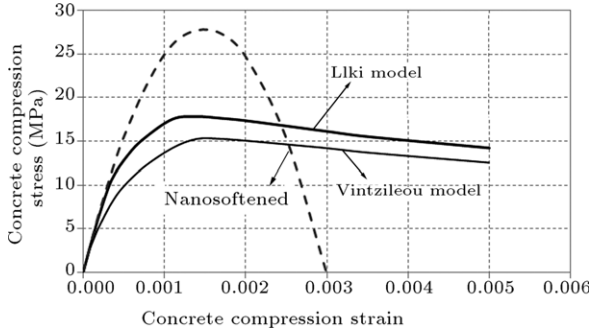


Figure 2: Stress–strain relationships of concrete in compression obtained by different models.

where:

$$H = \frac{4\bar{\varepsilon}_2}{\gamma_{lt} \sin 2\alpha_2} \quad (15)$$

A conditional term is then applied to control t_d , which must be smaller than the wall thickness in the case of hollow section beams.

2.3. Constitutive relationships of materials

The stress–strain relationship used in the proposed model is that developed by Belarbi and Hsu [17] for a softened compressive concrete, which was then modified by Chalioris [3] to include the effect of the FRP confinement by using the parameters proposed by Vintzileou and Panagiotidou [18] as follows:

$$\sigma_2^c = \sigma_p \left[2 \frac{\bar{\varepsilon}_2}{\varepsilon_p} - \left(\frac{\bar{\varepsilon}_2}{\varepsilon_p} \right)^2 \right] \quad \frac{\bar{\varepsilon}_2}{\varepsilon_p} \leq 1, \quad (16a)$$

$$\sigma_2^c = \sigma_p \frac{\bar{\varepsilon}_2}{\varepsilon_p} > 1, \quad (16b)$$

$$\sigma_p = k\zeta f'_c$$

$$\varepsilon_p = k^2 \zeta \varepsilon_0,$$

where f'_c is the concrete cylinder compressive strength, ε_0 is the concrete strain at the peak compressive stress taken as -0.00235 , ζ is the softening coefficient calculated from Eq. (17), and k is the FRP-confinement parameter, which is obtained from a simple empirical equation taken as Eq. (18):

$$\zeta = \frac{5.8}{\sqrt{f'_c (1 + 400\bar{\varepsilon}_1)}} \left(1 - \frac{|\beta|}{24^\circ} \right) \leq 0.9 \quad \text{and} \quad \frac{5.8}{\sqrt{f'_c}} \leq 0.9, \quad (17)$$

$$k = 1 + 1.3\alpha_n\omega_n,$$

$$\alpha_n = 1 - \frac{b^2 + h^2}{3A_c}, \quad (18)$$

$$\omega_n = \frac{\text{Volume of FRP material } f_{fu}}{\text{Volume of the confined concrete core } f'_c},$$

where β is the deviation angle taken as $0.5 \tan^{-1}(\gamma_{21}/(\varepsilon_2 - \varepsilon_1))$, and f_{fu} is the ultimate tensile strength of the FRP.

In Eq. (17), the softening coefficient, ζ , is applied for both strain and stress. However, the behavior of stress is different from strain, so two softened coefficients must be defined: one for stress (ζ_σ) and another for strain (ζ_ε). Ilki and Koc [19] modified the Belarbi and Hsu concrete model [17] to include the effect of FRP confinement by changing its descending branch.

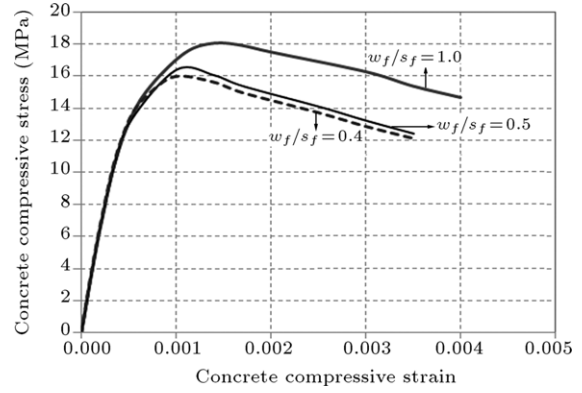


Figure 3: Compressive behavior of confined concrete in torsion for various configurations.

Finally, they represented stress and strain softening models as follows:

$$\zeta_\sigma = \frac{0.9}{\sqrt{1 + 400\bar{\varepsilon}_1}}, \quad (19a)$$

$$\zeta_\varepsilon = \frac{1}{\sqrt{1 + 500\bar{\varepsilon}_1}}. \quad (19b)$$

As in STM, the SMMT approach considers a uniform compressive stress across thickness t_d , rather than parabolic behavior, to make the procedure simpler. Therefore, an average stress factor, k_{1c} , is introduced by integration of the stress–strain relationships in Figure 2 as follows:

$$k_{1c} = \frac{1}{\bar{\varepsilon}_{2s}\sigma_p} \int_0^{\bar{\varepsilon}_{2s}} \sigma^c(\bar{\varepsilon}_2) d\bar{\varepsilon}_2$$

$$= \frac{\bar{\varepsilon}_{2s}}{k^2\zeta\varepsilon_0} - \frac{(\bar{\varepsilon}_{2s})^2}{3(k^2\zeta\varepsilon_0)^2} \frac{\bar{\varepsilon}_{2s}}{k^2\zeta\varepsilon_0} \leq 1 \quad (20)$$

$$k_{1c} = \frac{1}{\bar{\varepsilon}_{2s}\sigma_p} \int_0^{\bar{\varepsilon}_{2s}} \sigma^c(\bar{\varepsilon}_2) d\bar{\varepsilon}_2 = 1 - \frac{k^2\zeta\varepsilon_0}{3\bar{\varepsilon}_{2s}} \frac{\bar{\varepsilon}_{2s}}{k^2\zeta\varepsilon_0} > 1.$$

Consequently, the average compressive stress of the concrete struts is obtained by:

$$\sigma_2^c = k_{1c}\zeta f'_c. \quad (21)$$

The constitutive stress–strain laws for a plain compressive concrete, softened and FRP-confinement concrete models developed by Vintzileou and Panagiotidou [18] and Ilki and Koc [19] are shown in Figure 2. Furthermore, to understand the effect of FRP-confinement parameter, k , on the compressive behavior of concrete, stress–strain curves calculated from the proposed approach for continuous FRP full wrapping along the beam ($w_f/s_f = 1$) are obtained for strip FRP wrapping with ratios of $w_f/s_f = 0.5$ and $w_f/s_f = 0.4$ as shown in Figure 3.

The Belarbi and Hsu model [17] for the tensile stress–strain behavior of concrete in shear is modified by Jeng and Hsu [14] for torsion. The modifications include an increase in pre-cracking stiffness and strain at peak tensile stress. Finally, they represented the following equations:

$$\sigma_1^c = E_c \bar{\varepsilon}_1 \quad \text{for } \bar{\varepsilon}_1 \leq \varepsilon_{cr}$$

$$\sigma_1^c = f_{cr} \left(\frac{\varepsilon_{cr}}{\bar{\varepsilon}_1} \right)^{0.4} \quad \text{for } \bar{\varepsilon}_1 > \varepsilon_{cr}, \quad (22)$$

where: $E_c = 5620\sqrt{f'_c}$ (MPa), $\varepsilon_{cr} = 0.000116$ and $f_{cr} = E_c \varepsilon_{cr}$.

Contrary to STM and the CFT model, SMMT has successfully incorporated the effect of the tensile stress of concrete on torsional response, by defining an average stress factor for tensile stress similar to compressive stress. So, σ_1^c can be taken as Eq. (24) where k_{1t} , which is calculated by Eq. (25), is defined as the ratio of average tensile stress to peak tensile stress:

$$\sigma_{1c} = k_{1t} f_{cr} \quad (23)$$

$$k_{1t} = \frac{\bar{\varepsilon}_{1s}}{2\varepsilon_{cr}} \quad \text{for } \frac{\bar{\varepsilon}_{1s}}{\varepsilon_{cr}} \leq 1$$

$$= \frac{\varepsilon_{cr}}{2\bar{\varepsilon}_{1s}} + \frac{(\varepsilon_{cr})^{0.4}}{(0.6)\bar{\varepsilon}_{1s}} [(\bar{\varepsilon}_{1s})^{0.6} - (\varepsilon_{cr})^{0.6}] \quad \text{for } \frac{\bar{\varepsilon}_{1s}}{\varepsilon_{cr}} > 1. \quad (24)$$

According to determination of the shear modulus by Zhu and Hsu [20], concrete shear stress is related to shear strain as follows:

$$\tau_{21}^c = \frac{\sigma_1^c - \sigma_2^c}{2(\varepsilon_1 - \varepsilon_2)} \gamma_{21}. \quad (25)$$

The stress–strain relationship for steel bars, which is used in SMMT, is as follows:

$$f_s = E_s \bar{\varepsilon}_s \quad \text{for } \bar{\varepsilon}_s \leq \bar{\varepsilon}_n$$

$$f_s = f_y \left[(0.91 - 2B) + (0.02 + 0.25B) \frac{\bar{\varepsilon}_s}{\varepsilon_y} \right] \quad \text{for } \bar{\varepsilon}_s > \bar{\varepsilon}_n, \quad (26)$$

where:

$$B = (f_{cr}/f_y)^{1.5}/\rho \quad \text{and} \quad \bar{\varepsilon}_n = \varepsilon_y(0.93 - 2B).$$

FRP materials have a linear-elastic behavior up to failure based on tensile tests conducted by Deifalla [21]. Therefore, the constitutive model is a simple Hook's law equation as Eq. (27):

$$f_f = E_f \varepsilon_f \quad \text{for } \varepsilon_f \leq \varepsilon_{fe}, \quad (27)$$

where E_f is the Young's modulus of the FRP, and ε_f is the FRP effective tensile strain. Considering the mode of failure in FRP strengthening concrete beams, Deifalla and Ghobarah [22] proposed the three following formulas for determining effective tensile strain for debonding (Eq. (28)), peeling off (Eq. (29)), and rupture failure (Eq. (30)):

$$\varepsilon_{ef} = \frac{0.33 w_f}{L_e s_f}, \quad (28)$$

$$\varepsilon_{ef} = \frac{0.02 \alpha_f}{L_e}, \quad (29)$$

$$\varepsilon_{ef} = 0.1(E_f \rho_{ft})^{-0.86} \varepsilon_{f,\max}, \quad (30)$$

where $\varepsilon_{f,\max}$ is the maximum tensile strain of FRP, L_e is the effective bond length, and α_f is a constant parameter, which is used to take into account the difference in stress distribution between continuous FRP sheets and strips that are calculated by Teng et al. [23] formulas:

$$L_e = \sqrt{\frac{E_f t_f}{\sqrt{f_c'}}}, \quad (31)$$

$$\alpha_f = \sqrt{\frac{2 - \frac{w_f}{s_f \sin \beta_f}}{1 + \frac{w_f}{s_f \sin \beta_f}}}. \quad (32)$$

For the case of strengthening with U-jacketing FRP, Ghobarah does not give clear criteria for determining FRP effective strain.

Chalioris [3] adopted FIB [4] formulas for U-jacketing FRP strengthened beams as follows:

- If CFRP is used:

$$\varepsilon_{ef} = \min \left\{ \begin{array}{l} 0.17 \left(\frac{f_c^{2/3}}{E_f \rho_f} \right)^{0.3} \varepsilon_{fu} \\ 0.65 \left(\frac{f_c^{2/3}}{E_f \rho_f} \right)^{0.56} \times 10^{-3} \end{array} \right\}, \quad (33)$$

- If GFRP is used:

$$\varepsilon_{fe} = D_f \sigma_{f,\max} / E_f, \quad (34)$$

where:

$$\sigma_{f,\max} = \left\{ \begin{array}{l} f_{fu} \\ 0.427 \beta_L \beta_w \sqrt{\frac{E_f \sqrt{f_c'}}{t_f}} \end{array} \right\}, \quad (35a)$$

$$D_f = \left\{ \begin{array}{ll} \frac{2}{\lambda \pi} \frac{1 - \cos(\pi \lambda / 2)}{\sin(\pi \lambda / 2)} & \lambda \leq 1 \\ 1 - \frac{\pi - 2}{\pi \lambda} & \lambda > 1 \end{array} \right\}, \quad (35b)$$

$$\lambda = \frac{L_{\max}}{L_e} = \frac{0.9b}{\sqrt{E_f t_f / \sqrt{f_c'}}}; \quad (35c)$$

$$\beta_L = \left\{ \begin{array}{ll} 1 & \lambda \geq 1 \\ \sin(\pi \lambda / 2) & \lambda < 1 \end{array} \right\}; \quad \beta_w = \sqrt{\frac{2 - w_f / s_f}{1 + w_f / s_f}}, \quad (35d)$$

where E_f is in GPa and f_c is in MPa, according to FIB [4].

2.4. Solution algorithm

The solution technique of the proposed method, entitled SMMT–FRP, is an extension of the SMMT model. Two modifications have to be done in the SMMT algorithm:

- (1) The average stress factor, k_{1c} , on the descending branch of the stress–strain curve of compressive concrete is changed as presented in Eq. (20);
- (2) The convergence criteria for the solution procedure are obtained from equilibrium equations (Eq. (1)) by considering $\sigma_l = \sigma_t = 0$. So, FRP stress terms are added to the criteria used in the SMMT algorithm.

3. Model validation

The experimental data of 22 beams strengthened with FRP materials available from the literature are used to validate the proposed analytical model. The experimental studies are collected from the reported tests of Ghobarah et al. [2], Ameli et al. [10], Hii and Al-Mahaidi [12], Panchacharam and Belarbi [13] and Chalioris [8]. Hence, the accuracy of the model is checked based on real tests in a broad range of parametric studies. The beams used as databases had solid and hollow rectangular cross-sections, with longitudinal and transverse reinforcements of steel bars and stirrups, and strengthened with externally bonded CFRP or GFRP materials under various configurations; continuous and strip fabrics in complete wrapping or the U-jacketing scheme with fibers in transverse or longitudinal directions. Physical properties and strengthening configurations of beams are presented in Table 1.

Table 1: Physical properties of FRP strengthened RC beams.

Beam	Solid/hollow (t_w)	b/h (mm/mm)	f'_c	A_{st} (mm^2)	A_{st}/s (mm^2/mm)	f_{yt}, f_{yt} (MPa)	FRP mat. No. of Layers/Thickness	FRP configuration ^a
Ghobarah et al. [2]								
C1	Solid	150/350	37	603	0.452	409, 466	CFRP 1-layer/0.165 mm	W-C (t)
C2	Solid	150/350	37	603	0.452	409, 466	CFRP 1-layer/0.165 mm	W-S (t) $w_f/s_f = 0.5$
C4	Solid	150/350	37	603	0.452	409, 466	CFRP 1-layer/0.165 mm	W-S (t) $w_f/s_f = 0.67$
C5	Solid	150/350	37	603	0.452	409, 466	CFRP 1-layer/0.165 mm	W-S (t) $w_f/s_f = 0.4$
G1	Solid	150/350	37	603	0.452	409, 466	GFRP 1-layer/0.154 mm	W-C (t)
G2	Solid	150/350	37	603	0.452	409, 466	GFRP 1-layer/0.154 mm	W-S (t) $w_f/s_f = 0.5$
Ameli et al. [10]								
CFE	Solid	150/350	39	804	0.353	502, 251	CFRP 1-layer/0.165 mm	W-C (t)
CFE2	Solid	150/350	39	804	0.353	502, 251	CFRP 2-layer/0.165 mm	W-C (t)
CFS	Solid	150/350	39	804	0.353	502, 251	CFRP 1-layer/0.165 mm	W-S (t) $w_f/s_f = 0.5$
CJE	Solid	150/350	39	804	0.353	502, 251	CFRP 1-layer/0.165 mm	U-C (t)
CJS	Solid	150/350	39	804	0.353	502, 251	CFRP 1-layer/0.165 mm	U-S (t) $w_f/s_f = 0.5$
GFE	Solid	150/350	36	804	0.353	502, 251	GFRP 1-layer/0.154 mm	W-C (t)
GFE2	Solid	150/350	36	804	0.353	502, 251	GFRP 2-layer/0.154 mm	W-C (t)
Hii and Almahaidi [12]								
FS050D2	Solid	350/500	52.6	1100	0.226	398, 426	CFRP 2-layer/0.176 mm	W-S (t) $w_f/s_f = 0.29$
FH050D2	Hollow(50)	350/500	48.6	1100	0.226	398, 426	CFRP 2-layer/0.176 mm	W-S (t) $w_f/s_f = 0.29$
Panchacharam and Belarbi [13]								
A90W4	Solid	279/279	34	792	0.468	420 460, 420	GFRP 1-layer/0.154 mm	W-C (t)
A90S4	Solid	279/279	34	792	0.468	420 460, 420	GFRP 1-layer/0.154 mm	W-S (t) $w_f/s_f = 0.5$
C90U3	Solid	279/279	31	792	0.468	420 460, 420	GFRP 1-layer/0.154 mm	U-C (t)
A0L4	Solid	279/279	34	792	0.468	420 460, 420	GFRP 1-layer/0.154 mm	W-C (l)
A0L3	Solid	279/279	34	792	0.468	420 460, 420	GFRP 1-layer/0.154 mm	U-C (l)
Chalioris [8]								
RaS- FS150(2)	Solid	100/200	27.5	201	0.183	560 350	CFRP 2-layer/0.11 mm	W-S (t) $w_f/s_f = 0.5$
RbS- FS200(1)	Solid	150/300	28.8	201	0.238	560 350	CFRP 1-layer/0.11 mm	W-S (t) $w_f/s_f = 0.5$

^a W: wrapping; U: U-jacketing; C: continuous sheets; S: strip sheet (w_f/s_f : width/spacing of FRP sheets); t: fibers in transverse direction; l: fibers in longitudinal direction.

Comparisons between analytically predicted torque-twist curves and experimental ones are presented in Figure 4 for two beams tested by Chalioris [8], in Figures 5 and 6 for 6 beams tested by Ghobarah et al. [2], in Figure 7 for 6 beams tested by Ameli et al. [10], in Figure 8 for two tested beams of the Hii and Al-Mahaidi experimental study [12] and in Figure 9 for 6 beams tested by Panchacharam and Belarbi [13]. In addition, Figures 4 and 5 represent a comparative study of the results of the proposed model with those obtained by other researchers, which are available in Refs. [3,9]. Values of ultimate torque and the corresponding twist at ultimate torque, obtained from experimental tests, are compared with the analytical predicted ones in Table 2.

The difference between experimental results and torsion capacity calculated by the SMMT-FRP model has arisen from the following issues:

1. In the proposed model, the crack direction is taken as 45° with respect to longitudinal axes of the beam, even though the direction of cracks changes with an increase in torsion load, due to the existence of bar stress.
2. Material properties especially for concrete used in the analytical model are obtained from theories based on some simplifications and assumptions.

3. Experimental test results are highly sensitive to the accuracy of instruments. So, there would also be some errors in laboratory tests.

Based on the data presented in Table 2, reliable agreement between experimental results and outputs from the proposed model is proved. Note that, according to the author's efforts to obtain reliable results before the cracking stage for hollow beams, like FH050D2, in the proposed analytical model, the cracking strain of concrete should be decreased about 50%.

4. Comparison of proposed model with other analytical methods

Development of an analytical model based on the compression field theory for predicting the torsional capacity of strengthened RC beams was first implemented by Ameli and Ronagh [11]. This is a simple model, just capable of calculating the maximum torque that a strengthened RC beam could sustain. Chalioris [3] modified the Softened Truss Model to obtain both torsional capacity and the corresponding twist of maximum torque, in conjunction with FIB (2001) and the Teng failure criteria of FRP and the confined concrete model. This model employs the combination of two different theoretical models: smeared crack model and Softened Membrane Model (STM).

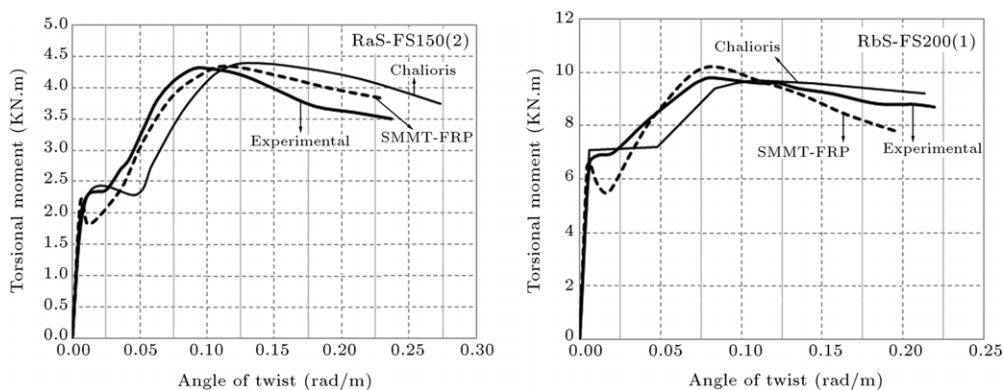


Figure 4: Comparison between results of the proposed model and Chalioris model for RaS-FS150(2) and RbS-FS200(1) [3].

Table 2: Ultimate torque and corresponding twist angle, obtained from experiments and calculated from SMMT–FRP.

Beam	$T_{cr,Exp}$	$T_{u,Exp}$	$\varphi_{u,Exp}$	$T_{cr,P}$	$T_{u,P}$	$\varphi_{u,P}$	$\frac{\varphi_{u,P}}{\varphi_{u,Exp}}$	$\frac{T_{cr,P}}{T_{cr,Exp}}$	$\frac{T_{u,P}}{T_{u,Exp}}$
Ghobarah et al. [2]									
C1	6.73	18.1	0.089	8.46	19.01	0.1014	1.139	1.257	1.050
C2	5.53	14.1	0.0916	7.59	16	0.0788	0.860	1.372	1.135
C4	6.57	16	0.0733	7.64	16.04	0.0733	1.00	1.163	1.002
C5	5.87	13.6	0.0707	7.59	15.85	0.071	1.003	1.293	1.165
G1	7.17	18.9	0.105	7.40	19.94	0.125	1.190	1.032	1.055
G2	6.29	13.2	0.084	7.59	15.98	0.080	0.956	1.207	1.210
Ameli et al. [10]									
CFE	10.4	28	0.137	11.37	23.85	0.114	0.835	1.093	0.852
CFE2	10.7	36.5	0.193	10.84	28.15	0.167	0.865	1.013	0.771
CFS	10.3	21.7	0.0982	10.56	19.96	0.100	1.018	1.025	0.919
GFE	9.7	26.3	0.144	10.47	24.14	0.132	0.917	1.079	0.918
GFS	10.5	19.9	0.0884	10.56	20	0.100	1.131	1.006	1.005
Hii and Almahaidi [12]									
FS050D2	73.7	89	0.102	67.38	84.02	0.097	0.950	0.914	0.944
FH050D2	21.3	86	0.104	27.8	78.46	0.097	0.932	1.305	0.912
Panchacharam and Belarbi [13]									
A90W4	22	45.00	0.06	24.42	42.31	0.057	0.95	1.11	0.942
A90S4	21	34.00	0.100	22.05	34.30	0.088	0.88	1.05	1.013
C90U3	20	24.00	0.028	18.2	26.38	0.024	0.86	0.91	1.103
A0L4	26	29.00	0.048	24.78	32.42	0.040	0.83	0.95	1.127
A0L3	25	26.00	0.032	31.98	28.78	0.040	1.25	1.28	1.114
Chalioris [8]									
RaS-FS150(2)	2.35	4.33	0.098	2.19	4.35	0.117	1.194	0.932	1.005
RbS-FS200(1)	6.93	7.52	0.08	7.1	10.19	0.077	0.963	1.025	1.355
							Mean = 0.98	1.101	1.030

Exp.: experimental result
P: proposed model result
u: ultimate torque or twist
cr: cracking torque or twist.

The former is used in the pre-cracking stage and the latter in post-cracking. To compare the proposed model (extension of SMMT) with the Chalioris model (extension of STM), specimens RaS-FS150(2) and RbS-FS200(1) are run through SMMT–FRP. The curves obtained by the proposed model are shown in Figure 4 beside the Chalioris predicted curves. The more reliable results are obtained from the proposed model in comparison with Chalioris results, which were not capable of predicting the nonlinear stage of the torsional behavior of beams as well as SMMT–FRP.

Ghobarah and Deifalla [9] developed a new analytical model based on the Modified Compression Field Theory (MCFT), the hollow tube analogy, and the compatibility at the corner of

the cross section to draw the entire torque-twist curve of a RC beam wrapped with FRP. A comparative study is implemented to compare the proposed model (SMMT–FRP) with the results of Ghobarah and Deifalla [9] for experimental curves of Ref. [2] as shown in Figure 5. It can be concluded from similar torque-twist curves of two models in Figure 5, with many coinciding points, that SMMT–FRP and the Ghobarah and Deifallah model will lead to similar results in FRP-strengthening cases. The proposed model will predict the full torsional behavior of RC beams strengthened with FRP during an algorithm consisting of two trial and error loops, while the Ghobarah solution includes four trial and error loops. Therefore, the biggest advantage of the proposed model is its time efficiency compared to the

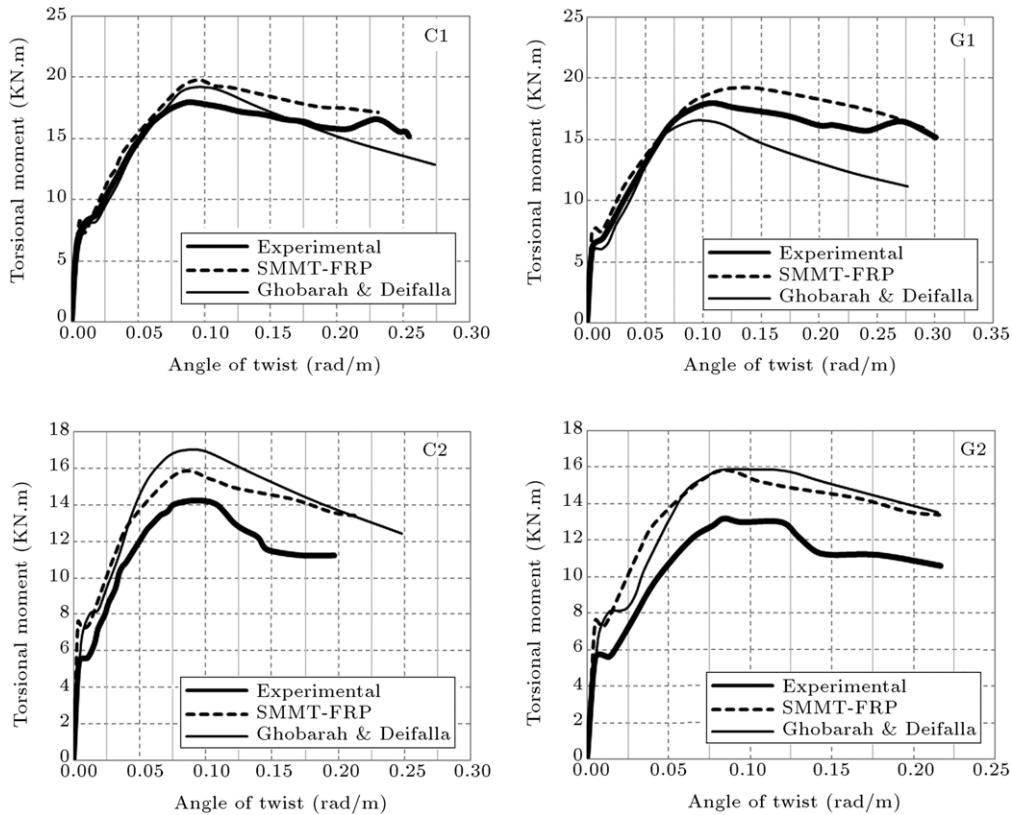


Figure 5: Comparison between the calculated curves obtained from the proposed model and Ghojarah and Deifalla model with experimental results for beams C1, C2, G1 and G2 [9].

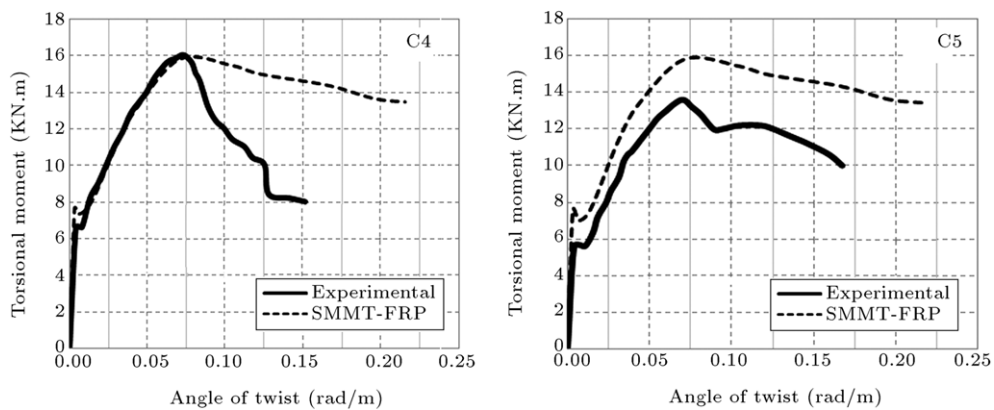


Figure 6: Comparison between outputs of the proposed model with experimental curves for beams C4 and C5 tested by Ghojarah et al. [2].

Ghojarah model. Moreover, Table 3 comprises comparative ratios of ultimate torsional moments that were obtained from the proposed model, and the ones calculated by other analytical models for various experimental tests.

5. Contribution of FRP fabrics to the torsional capacity

Previous comparisons between experimental and analytical torque-twist curves proved that the proposed analytical model provides a reliable assessing tool for predicting the entire torsional behavior of FRP strengthening beams.

The contribution of FRP fabrics could be simplified as the difference between the measured ultimate torque moment of

the strengthened beams and the maximum torsional moment capacity of the respective control beam [8]. These values are given in Table 4 in terms of torsional moment (T_f). In Table 4, experimental specimens tested by Ghojarah et al. [2] are extended to other strengthening configurations including U-jacketing and 2 layer FRP sheets for each strengthening scheme.

Based on the values of T_f and the characteristics of FRP patterns, the effective strain of the fibers (ε_{ef}) has been calculated by the following expression [13]:

In the case of Wrapping FRP fabric:

$$\varepsilon_{ef} = \frac{T_f s_f}{2 A_0 A_f E_f} \quad (36a)$$

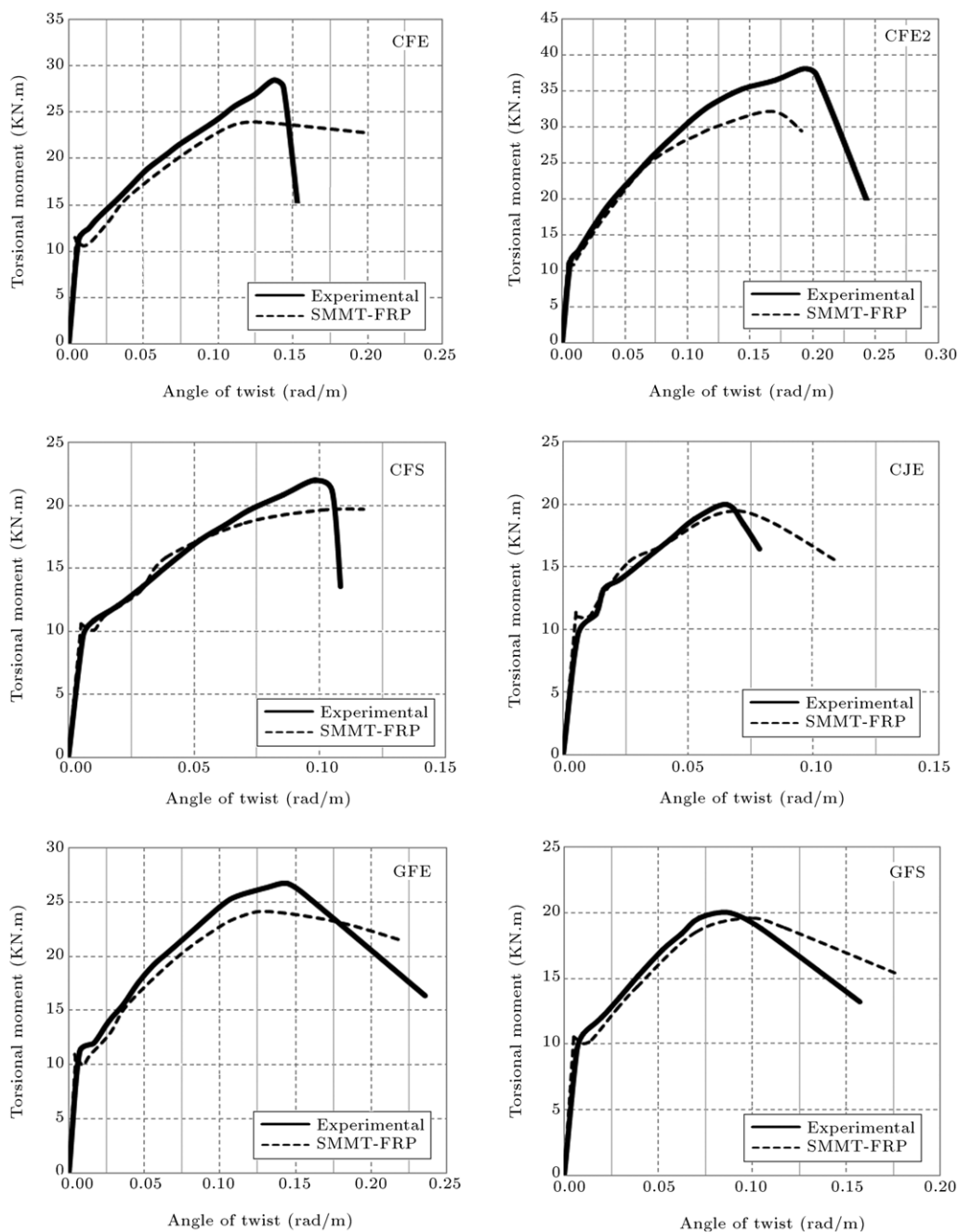


Figure 7: Comparison between outputs of the proposed model with experimental curves for beams strengthened by CFRP (CFE, CFE2, CFS and CJE) and GFRP (GFE and GFS) tested by Ameli et al. [10].

In the case of U-jacketing:

$$\varepsilon_{ef} = \frac{T_f s_f}{A_0 A_f E_f}, \quad (36b)$$

where A_0 is the gross area enclosed by the shear-flow path within the FRP fabric.

On the other hand, ε_{ef} can be calculated using Eqs. (28) to (34), which is shown by ε_{ef-Cal} in Table 4. Furthermore, a comparative study between ε_{ef-Cal} and ε_{ef} is performed in Table 4.

The effective strain of the fibers could be assumed as an index for the effectiveness of the FRP fabrics, since it represents the rate of fiber utilization in each test [8]. According to

experimental observations, two main modes of failure were observed as represented in Table 4. In the case of fully wrapped strengthened beams along the entire beam, the FRP rupture was reported by Ameli et al. [10] and Panchacharam and Belarbi [13], while for similar beams tested by Ghojarah [2], the concrete fractured before the FRP rupture. For beams strengthened by FRP strips, the FRP rupture was found in [10,13] experiments, and debonding was reported by Ghojarah et al. [2]. For beams with U-jacketing configuration, debonding failure was observed in [10,13] experiments.

Considering the linear behavior for FRP materials, the failure strain of the FRP is calculated from the division of ultimate stress under the elastic modulus of FRP. In this way, the failure

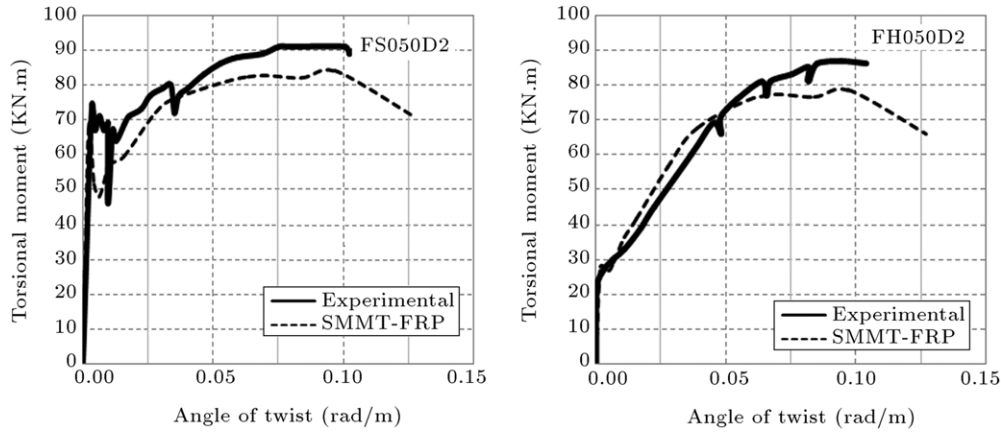


Figure 8: Comparison between outputs of the proposed model with experimental curves for the solid (FS050D2) and hollow (FH050D2) beams tested by Hii and Al-Mahaidi [12].

Table 3: Comparison between torsional capacity calculated by proposed model (T_P), Ameli model (T_{Ameli}), Ghobarah model ($T_{Ghobarah}$) and Chaliors model ($T_{Chaliors}$).

Beam	T_{Ameli} [11]	$T_{Ghobarah}$ [9]	$T_{Chaliors}$ [3]	T_P	T_P/T_{Ameli}	$T_P/T_{Ghobarah}$	$T_P/T_{Chaliors}$
Ghobarah et al. [2]							
C1	16.70	19.00	19.45	19.01	1.14	1.00	0.98
C2	15.90	17.00	16.65	16.00	1.01	0.94	0.96
C4	–	16.00	17.37	16.04	–	1.00	0.92
C5	–	–	16.01	15.85	–	–	–
G1	15.30	17.90	18.38	19.94	1.30	1.11	1.08
G2	14.80	16.00	16.42	15.98	1.08	1.00	0.97
Ameli et al. [10]							
CFE	23.10	–	25.28	23.85	1.03	–	0.94
CFE2	26.10	–	30.42	28.15	1.08	–	0.93
CFS	21.80	–	22.09	19.96	0.92	–	0.90
GFE	19.60	–	18.71	24.14	1.23	–	1.29
GFS	19.30	–	20.05	20.00	1.04	–	1.00
Hii and Almahaidi [12]							
FS050D2	–	–	93.24	84.02	–	–	0.90
FH050D2	–	–	–	78.46	–	–	–
Panchacharam and Belarbi [13]							
A90W4	–	–	44.64	42.31	–	–	0.95
A90S4	–	–	35.20	34.30	–	–	0.97
C90U3	–	–	28.33	26.38	–	–	0.93
A0L4	–	–	29.34	32.42	–	–	1.10
A0L3	–	–	27.15	28.78	–	–	1.06
Chaliors [8]							
RaS-FS150(2)	–	–	4.40	4.35	–	–	0.99
RbS-FS200(1)	–	–	9.69	10.19	–	–	1.05

strains of CFRP and GFRP used in Ameli et al. [10] experiments, are 0.016 and 0.046, respectively, while the effective strain obtained from Eq. (36), presented in Table 4, is further from FRP failure strain. This illustrates that the effective strain of FRP is only a practical criteria for analytical models. Previous analytical approaches [3,9,11] and the proposed model in this paper used the effective strain as a parameter for omitting the effect of FRP from equilibrium equations. The presented torque-twist curves in Figs. 4 to 9 show that the effective strain obtained from Eqs. (28) to (34) controls the torsional capacity of the FRP strengthened beams.

Applying Chaliors criteria [3] for calculating the effective strain of FRP in U-jacketing configuration leads to an extension of the strengthening configuration of beams

tested by Ghobarah [2] with the U-jacketing strengthening scheme. A comparison of torsional capacities of extended Ghobarah models with experimental tested beams with the same strengthening configuration (U-jacketing), considered by Ameli et al. [10], shows the reasonable results of the proposed model in this case of strengthening. To validate the proposed model in the case of U-jacketing, comparison between the predicted decrease in torsional capacity and that experimentally tested by Ameli et al. [10] is presented in Table 5. With respect to Table 5, strengthening beams with U-jacketing configuration show 10% up to 20% decrease in torsional capacity.

Moreover, to study the effect of the number of layers in torsional capacity, 4 beams of Ghobarah et al. [2] experiments, which were strengthened with one-layer FRP fabric (C1, C2,

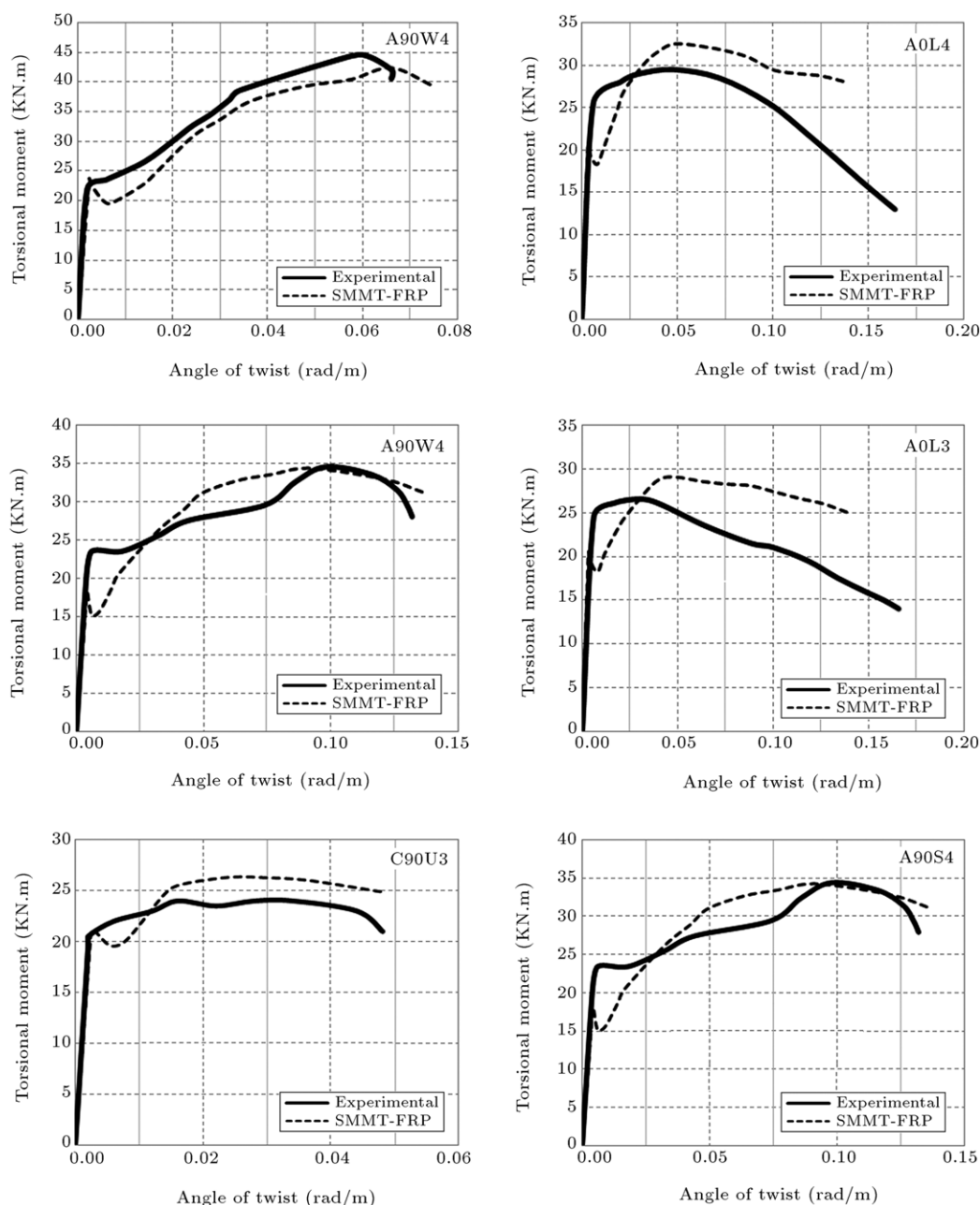


Figure 9: Comparison between outputs of the proposed model with experimental curves for beams tested by Panchacharam and Belarbi [13].

G1 and G2), are analytically strengthened by two-layer FRP under the proposed model. Table 6 consists of the torsional moment capacity of experimental beams strengthened with a 1-layer FRP sheet and those strengthened by 2-layer FRP and obtained by analytical procedure. Considering Table 6 results, it is obvious that both analytical models and experimentally tested beams of Ameli et al. [10], strengthening by the 2-layer FRP sheet makes the torsional capacity increase up to approximately 30% and 5% for continuous and strip wrapping configurations, respectively.

6. Conclusion

The full torsional behavior of FRP strengthened RC solid and hollow rectangular beams is predicted by a rational model

developed in this paper, which is an extension of SMMT. The proposed model is capable of calculating the compressive and tensile strain of concrete, as well as the tensile strain in FRP and steel bars. The model accounts for several possible strengthening techniques, including CFRP and GFRP complete wrapping, spiral strips, complete U-jacketing along the beam, and U-jacketing strips. By validating the results obtained from the proposed model by experimentation, reasonable agreement of this model for predicting the torsional behavior of RC beams strengthened with FRP fabrics is shown.

The results of this study show that the torsional capacity of beams strengthened by U-jacketing fabrics decreases up to 20%, with respect to full wrapping configuration. On the other hand, by using 2 layers of FRP fabric instead of 1, torsional capacity

Table 4: Study on contribution of FRP fabrics on torsional capacity.

Model name	FRP material	T_u	T_f	ε_{ef}	ε_{ef-cal}	$\varepsilon_{ef-cal}/\varepsilon_{ef}$	Mode of failure
Ghobarah et al. [2]							
C1	CFRP	19.01	8.01	0.0019	0.0022	1.11	N.A.
C1-2Layer ^a	CFRP	25.62	14.62	0.0018	0.0028	1.57	N.A.
C1-U ^a	CFRP	16.84	5.84	0.0029	0.0032	1.12	Debonding
G1	GFRP	19.94	8.94	0.003	0.0043	1.26	N.A.
G1-2Layer ^a	GFRP	25.62	14.62	0.0027	0.0033	1.20	N.A.
G1-U ^a	GFRP	16.52	5.52	0.0041	0.0039	0.95	Debonding
C2	CFRP	16	5	0.0024	0.0034	1.405	Debonding
C2-2Layer ^a	CFRP	17.05	6.05	0.0015	0.0014	0.95	Debonding
C2-U ^a	CFRP	13.51	2.51	0.0025	0.0033	1.34	Debonding
G2	GFRP	15.98	4.98	0.0037	0.0058	1.56	Debonding
G2-2Layer ^a	GFRP	16.76	5.76	0.0021	0.0017	0.79	Debonding
G2-U ^a	GFRP	14.85	3.85	0.0058	0.0043	0.83	Debonding
Ameli et al. [10]							
CFE	CFRP	23.85	8.85	0.0022	0.0041	1.22	FRP rupture
CFE2	CFRP	28.15	13.15	0.0016	0.0029	1.15	FRP rupture
CJE	CFRP	19.67	4.67	0.0023	0.0033	1.33	Debonding
GFE	GFRP	24.14	9.34	0.0070	0.0077	1.10	FRP rupture
GFE2	GFRP	31.1	16.3	0.0030	0.0033	1.07	FRP rupture
GJE	GFRP	19.5	4.7	0.0035	0.0032	0.93	Debonding
CFS	CFRP	21.7	6.9	0.0033	0.0020	0.61	FRP rupture
CJS	CFRP	17.4	2.6	0.0025	0.0032	1.33	Debonding
GFS	GFRP	19.9	5.1	0.0038	0.0038	0.99	FRP rupture
GJS	GFRP	16.9	2.1	0.0031	0.0045	1.23	Debonding
Panchacharam and Belarbi [13]							
A90W4	GFRP	45	27	0.0068	0.005647	0.83	FRP rupture
A90S4	GFRP	34	16	0.0081	0.009032	1.12	FRP rupture
C90U3	GFRP	24	6	0.0030	0.004143	1.37	Debonding
A0L4	GFRP	29	11	0.0055	0.009203	1.66	–
A0L3	GFRP	26	8	0.0040	0.005726	1.42	–
Chalioris [8]							
RaS-FS150(2)	CFRP	4.33	1.92	0.0038	0.004667	1.23	–
RbS-FS200(1)	CFRP	7.52	2.65	0.0047	0.005447	1.17	–

^a Beams are analyzed by proposed analytical model and they are not studied experimentally.

Table 5: Comparison between torsional capacities for beams strengthened with U-jacketing and wrapping configuration.

Beam	Configuration		Decreasing (%)
	Wrapping	U-Jacketing	
Ghobarah et al. [2]			
C1	19.01	16.84	–11.4
G1	19.94	16.52	–17.2
C2	16	13.51	–15.6
G2	15.98	14.85	–7.1
Ameli et al. [10]			
CFE	23.85	19.67	–17.5
GFE	24.14	19.5	–19.2
CFS	21.7	17.4	–19.8
GFS	19.9	16.9	–15.1

Table 6: Comparison between torsional capacities for beams strengthened with 2-layer and 1-layer FRP.

Beam	Configuration		Increasing (%)
	1-layer	2-layer	
Ghobarah et al. [2]			
C1	19.01	25.62	34.8
G1	19.94	25.62	28.5
C2	16.	17.05	6.6
G2	15.98	16.76	4.9
Ameli et al. [10]			
CFE	23.85	28.15	18.0
GFE	24.14	31.1	28.8

increases up to 30% for full wrapping and 6% for strip wrapping strengthening configuration.

The effective strain of the fibers, as an index for the effectiveness of the FRP fabrics, was calculated by combinative relationships available in literature. The calculated maximum FRP strains for experimentally tested beams are compared with the proposed model. The results of the calculated effective strains were 0.8 up to 1.4 times the experimentally measured ones. Hence, more experimental studies are needed to be conducted for proposing more reliable relationships for calculating effective strain.

References

- [1] Kozonis, D. "Strength evaluation and retrofit of reinforced concrete beams subjected to pure torsion", M.Sc. Thesis, Department of Civil Engineering, RICE University, Huston, Texas (1997).
- [2] Ghobarah, A., Ghorbel, M.N. and Chidiac, S.E. "Upgrading torsional resistance of reinforced concrete beams using fiber-reinforced polymer", *Journal of Composites for Construction*, 6(4), pp. 257–263 (2002).
- [3] Chalioris, C. "Analytical model for torsional behavior of reinforced concrete beams retrofitted with FRP materials", *Engineering Structures*, 29(12), pp. 3263–3276 (2007).
- [4] FIB, "Externally bonded FRP reinforcement for RC structures", CEB-FIP, Technical Report, 14, pp. 59–68 (2001).
- [5] JSCE concrete engineering series 41, "Recommendations for Upgrading of Concrete Structures with Use of Continuous Fiber Sheets" (2001).

- [6] ACI Committee 318, "Building Code Requirement for Structural Concrete and Commentary", American Concrete Institute, Detroit, MI, USA (1999).
- [7] CSA S806, "Design and Construction of Building Components with Fiberreinforced Polymers", Canadian Standards Association, Toronto, Ontario, Canada (2002).
- [8] Chalioris, C. "Torsional strengthening of rectangular and flanged beams using carbon fibre reinforced-polymers—experimental study", *Construction & Building Materials*, 22(1), pp. 21–29 (2008).
- [9] Deifala, A.F. and Ghobarah, A. "Full torsional behavior of RC beams wrapped with FRP: analytical model", *Composites for Construction*, 14(3), pp. 289–300 (2010).
- [10] Ameli, M., Ronagh, H.R. and Dux, P.F. "Behavior of FRP strengthened reinforced concrete beams under torsion", *Composites for Construction*, 11(2), pp. 192–200 (2007).
- [11] Ameli, M. and Ronagh, H.R. "Analytical method for evaluating ultimate torque of FRP strengthened reinforced concrete beams", *Composites for Construction*, 11(4), pp. 384–390 (2007).
- [12] Hii, A.K.Y. and Al-Mahaidi, R. "An experimental and numerical investigation on torsional strengthening of solid and box-section RC beams using CFRP laminates", *Composite Structures*, 75, pp. 213–221 (2006).
- [13] Panchacharam, S. and Belarbi, A. "Torsional behavior of reinforced concrete beams strengthened with FRP composites", in: *Proceedings 1st FIB congress*, Japan (2002).
- [14] Jeng, C.H. and Hsu, T.T.C. "A softened membrane model for torsion in reinforced concrete members", *Engineering Structures*, 31(9), pp. 1944–1954 (2009).
- [15] Jeng, C.H. "Simple rational formulas for cracking torque and twist of reinforced concrete members", *ACI Structural Journal*, 107(19), pp. 189–197 (2010).
- [16] Hsu, T.T.C. and Zhu, R.R.H. "Softened membrane model for reinforced concrete elements in shear", *ACI Structural Journal*, 99(4), pp. 460–469 (2002).
- [17] Belarbi, A. and Hsu, T.T.C. "Constitutive laws of softened concrete in biaxial tension-compression", *ACI Structural Journal*, 92(5), pp. 562–573 (1995).
- [18] Vintzileou, E. and Panagiotidou, E. "An empirical model for predicting the mechanical properties of FRP-confined concrete", *Construction & Building Materials*, 22(8), pp. 841–854 (2008).
- [19] Ilki, A.K.N. and Koc, V. "Low strength concrete members externally confined with FRP sheets", *Structural Engineering and Mechanics*, 18(2), pp. 167–194 (2004).
- [20] Zhu, R.R.H., Hsu, T.T.C. and Lee, J.Y. "Rational shear modulus for smeared crack analysis of reinforced concrete", *ACI Structural Journal*, 98(4), pp. 343–350 (2001).
- [21] Deifala, A.F. "Behavior and strengthening of RC T-girders in torsion and shear", Ph.D. Thesis, Department of Civil Engineering, McMaster University, Hamilton, Ontario, Canada (2007).
- [22] Deifala, A.F. and Ghobarah, A. "Simplified analysis for torsionally strengthened RC beams using FRP", in: *Proceeding of the International Symposium on Bond Behavior of FRP in Structures, BBFS 2005*, International Institute for FRP in construction (2005).
- [23] Teng, J.G., Chen, J.F., Smith, S.T. and Lam, L., *FRP Strengthened RC Structures*, Wiley, Chichester, UK (2002).

Alireza Zojaji received his B.S. degree from Iran University of Science and Technology and his M.S. degree from Amirkabir University of Technology, Iran. His research interests include composite structures, structural analysis using FEM, analytical methods in structural engineering, and damage detection, especially in the composite structures and rehabilitation of structural members using FRP materials.

Mohammad Z. Kabir is Associate Professor in the Department of Civil and Environmental Engineering at Amirkabir University of Technology, Tehran, Iran, from where he received his B.S. and M.S. degrees. He received his Ph.D. degree from Waterloo University in Canada. His research interests include structural stability, structural analysis using FEM, experimental methods in structural engineering, composite structures, structural optimization, damage detection and rehabilitation of structures.